

2016

The Reconfigurable Machinery Efficient Workspace Analysis Based on the Twist Angles

Ana M. Djuric


Vukica Jovanovic

Old Dominion University, v2jovano@odu.edu

Mirjana Filipovic

Ljubinko Kevac

Follow this and additional works at: https://digitalcommons.odu.edu/engtech_fac_pubs

 Part of the [Artificial Intelligence and Robotics Commons](#), [Industrial Engineering Commons](#), [Industrial Technology Commons](#), [Manufacturing Commons](#), and the [Operational Research Commons](#)

Repository Citation

Djuric, Ana M.; Jovanovic, Vukica; Filipovic, Mirjana; and Kevac, Ljubinko, "The Reconfigurable Machinery Efficient Workspace Analysis Based on the Twist Angles" (2016). *Engineering Technology Faculty Publications*. 13.
https://digitalcommons.odu.edu/engtech_fac_pubs/13

Original Publication Citation

Djuric, A. M., Jovanovic, V., Filipovic, M., & Kevac, L. (2016). The reconfigurable machinery efficient workspace analysis based on the twist angles. *International Journal of Computer Applications in Technology*, 53(2), 201-211. doi:10.1504/IJCAT.2016.074460

The reconfigurable machinery efficient workspace analysis based on the twist angles

Ana M. Djuric*, Vukica Jovanovic,
Mirjana Filipovic and Ljubinko Kevac

Engineering Technology Division,
College of Engineering,
Wayne State University,
5050 Anthony Wayne Dr.,
Detroit, MI 48202, USA
Email: ana.djuric2@wayne.edu
Email: v2jovano@odu.edu
Email: mira@robot.imp.bg.ac.rs
Email: ljubinko.kevac@gmail.com

*Corresponding author

Abstract: A novel methodology for the calculation, visualisation and analysis of the Reconfigurable Machinery Efficient Workspace (RMEW), based on the twist angles, is presented in this paper. The machinery's kinematic parameters are used for calculating the workspace, while the efficient workspace is associated with the machinery's path and includes the end-effector position and orientation. To analyse and visualise many different machinery efficient workspaces at the same time, the calculation is based on the previously developed and validated complex reconfigurable machinery's kinematic structure named n -DOF Global Kinematic Model (n -GKM). An industrial robot is used as an example to demonstrate an application of n -GKM model. It is calculated only for the tool's perpendicular orientation relative to the floor. Four different kinematic configurations based on twist angles (α_i) were selected to demonstrate the outcomes. Their graphical representations show how the twist angles significantly affect the shape and size of the efficient workspace. RMEW can be used as a design tool for new machinery's kinematic structure and layout design. This methodology can be applied for any tool orientation.

Keywords: industrial robotics; workplace analysis.

Reference to this paper should be made as follows: Djuric, A.M., Jovanovic, V., Filipovic, M. and Kevac, L. (2016) 'The reconfigurable machinery efficient workspace analysis based on the twist angles', *Int. J. Computer Applications in Technology*, Vol. 53, No. 2, pp.201–211.

Biographical notes: Ana M. Djuric is an Assistant Professor of Engineering Technology in the College of Engineering at Wayne State University (WSU). Her research areas are industrial robots, kinematics, dynamics, control and advanced manufacturing systems. She has published over 30 journal and conference papers. Prior to her arrival at WSU, she worked in the industry for five years. She worked as a Machine and Tool Designer first and then as a Robotics Software Analyst. She worked as an Instructor for four years at the Mechanical, Automotive, Materials, and Industrial and Manufacturing Systems Engineering departments at the University of Windsor.

Vukica Jovanovic is an Assistant Professor in the Mechanical Engineering Technology Department at the Frank Batten College of Engineering and Technology at Old Dominion University in Norfolk, VA. Her research focuses on mechatronics, product identification, product life cycle management, assembly systems, automation and energy efficiency. Previously, she worked in the engineering services, aerospace and power generation industries. She taught at Trine University in Angola, IN, in the Design Engineering Technology Department. Before Trine, she was a Graduate Research Assistant at Purdue University in the Product Lifecycle Management Center of Excellence. She also worked as Faculty at the University of Novi Sad in the Industrial Engineering Department.

Mirjana Filipovic is an Associate Research Professor at Mihajlo Pupin Institute, University of Belgrade. Her research areas include robotics, industrial, humanoid, cable-suspended parallel robots, with and without elasticity elements, theory of non-linear systems, controls and programming. She has published ten international journal papers and 28 international conference papers. Until 1991, her major concerns were engineering assignments and projects for the 'Center for Pneumatics in Belgrade'.

Ljubinko Kevac is a Research Assistant and a PhD Student at the Innovation Center, School of Electrical Engineering at the University of Belgrade. His research areas are cable-suspended parallel robots, controls, dynamics and kinematics of robotic mechanisms. He has published over 15 journal and conference papers. During his BS studies, he had an Internship at Manipal University of Technology in Karnataka, India, in the Control Systems Department.

1 Introduction

There is a need for the development and implementation of reconfigurable manufacturing systems in today's highly changeable market (Koren, and Shpitalni, 2010). Products are constantly getting more customised and product life cycles shorter (Haque, 2012). Hence, there is a demand for smarter, more reconfigurable manufacturing systems which can hold up to that need. However, to be reconfigurable and automated at the same time is not an easy task. It relies on heavy engineering processes and the development of new machine configurations and layouts even before the system gets reconfigured. There is no time to experiment and halt the production until the perfect combination is achieved. For that purpose, a more automated approach to calculation, visualisation and analysis of efficient workspaces, machine configurations and decision-making support is required. The key of any manufacturing system is automation which requires the coordination of different machines to support manufacturing operations in a company. An automated design tool for the design and optimisation of kinematic structures for new numerically controlled machines is needed to enable complex manufacturing systems with reconfigurable characteristics.

Various manufacturers are focusing on the development of new methods related to the improvement of robot performance, cost reductions and new efficiencies through multi-robot control, safe control, force control, 3D vision, remote robot supervision and wireless communication (Brogårdh, 2007). Many of these problems are important for mobile robotics (Yan et al., 2012). They are the basis of flexible automation which enables mechatronic systems to act according to the changes which are frequently happening in manufacturing systems (Guerra-Zubiaga et al., 2010). Accurate and robust mathematical modelling is usually the start of any design of new machinery. In mechatronic design, both mechanical and control systems are designed in an integrated approach (van Amerongen and Breedveld, 2003). The preferred structure and parameters should be directly associated with the physical components. One of the main aspects of any mechatronic system is the mechanical system. In this paper, the authors are focusing on an example of an industrial robot and one mathematical approach for determining an optimal workspace.

2 Machinery workspace and efficient workspace

A mechanical system and its accurate mapping is usually the starting point in understanding how robots can be designed and used in manufacturing systems. Model-based

control leads to control schemes that deliver greater performance. This may be in conflict with the cost reduction and optimisation design strategies. There is a trend leading to more complex kinematic and dynamic models' Multiple-Input and Multiple-Output (MIMO) control schemes, variations of static and dynamic model parameters, increasing noise and disturbance levels, a larger number of low mechanical eigenfrequencies and enlarged non-linearities (Brogårdh, 2007). This all leads to the need for more careful mathematical modelling related to various conditions and situations which may happen in a manufacturing cell and that are directly related to the robot workspace.

The automated machines, such as industrial robots, are designed with various parameters such as number of Degrees of Freedom (DOF), link lengths, link offsets, joint types, payloads, desired accuracy, available workspace, singular space, etc. All of these constraints are the key elements that serve as a basis for the cell layout design. The kinematics and the related parameters are used for calculation of the machinery workspace and efficient workspace and they are dependent on the machine's path (Djuric and Urbanic, 2009). It is very important to determine the 3D design envelope which would contain space for all of the industrial robot's trajectories, considering positions with possible DOF and its angle limitations. This problem is important from multiple points of view: production design, safety engineering, path analysis, robot programming and layout design. The machine trajectory is basically a series of connected points in 3D space, a 3D sketch, which is built from points, representing joints, and lines, representing links. Each point is defined with its relative position and orientation (a vector) related to the machinery's base frames or pre-defined user frame (absolute position).

The robot moves from point to point using the desired motion type (linear, arc or joint). Trajectory planning has two phases, the first of which is to check for machinery, if it can reach the selected part(s). This operation can be simply done by placing the part(s) inside the machinery's workspace.

Machinery workspace. The machinery's workspace represents a set of all reachable points by the tool frame without considering their orientation (Djuric and ElMaraghy, 2008). To visualise the machinery's workspace, many available tools can be used. It is common that some of the accessible points cannot be reached with the desired tool orientation, even though it falls inside the workable space. For that purpose, an accurate and optimal machinery path

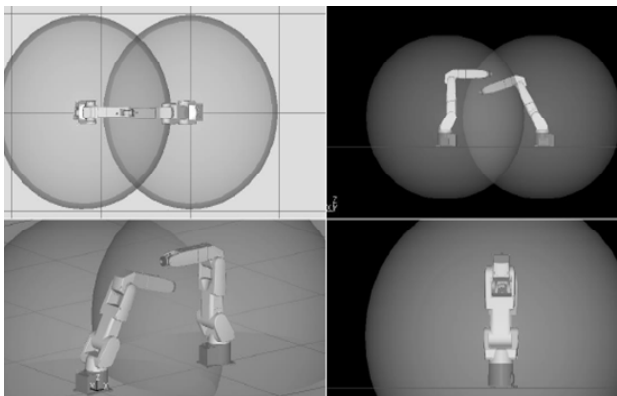
generation along with visualisation is highly needed for successful use of pre-determined regions related to the application. These regions are named the machinery's work window.

Efficient workspace. The basic calculations of one single kinematic structure in efficient workspace were previously done by several researchers (Djuric et al., 2013a; Djuric et al., 2013b; Djuric et al., 2013c). They investigated workspace boundaries for different DOF, joint types and kinematic structures utilising various approaches (Castelli et al., 2008; Cebula and Zsombor-Murray, 2006; Ceccarelli and Lanni, 2003; Yang et al., 2009).

Previous research introduced a basic definition of the efficient workspace and has not resulted in any analysis of its shape as it relates to the robot's twist angle. In the comparison of all 6R robot kinematic structures, the main difference is in their joint positive directions which are determined with their twist angles. This motivates the researchers to analyse the influence of the twist angles to the shape of the efficient workspace when the tool is perpendicular. Results of this study could be used as a design tool for new robots' kinematics and their integration in a multiple robot work cell. This workspace analysis is very important for safety purposes in the production.

Many industrial robots work together in manufacturing systems and share their workspaces in the same space, as shown in Figure 1 (Curkovic et al., 2013). Hence, management of their efficient workspace is important for their successful management.

Figure 1 Two robot workspaces in 3D



Source: Curkovic et al. (2013)

3 Industrial robot Fanuc LR Mate 200iC

An industrial robot which was used for this study, as an example, is an electric, servo-driven mini-robot. It is a table-top size robot designed for the following operations: machine tending, material handling, assembly, picking and packing, part washing, material removal, dispensing, testing and sampling, and for education and entertainment (Fanuc, 2009). This robot has six DOF, can lift up to 5 kg at the

wrist and it can flip over backwards for a larger work envelope. It can also work in high-speed applications and can be controlled via standard Ethernet or through ladder-logic-controlled peripheral devices. Its links are driven by a brushless AC motor and 110 VAC single-phase input voltage. Its J1 axis can revolve full circle. The compact design of this robot makes it convenient for various applications such as the one shown in Figure 2 when this robot was used at the Max Planck Institute for Plasma Physics (IPP) in Greifswald, Germany, for the inner walls of the fusion reactor (Foitzik, 2012).

Figure 2 Fanuc LR Mate 200iC in a welding application



Source: Foitzik (2012)

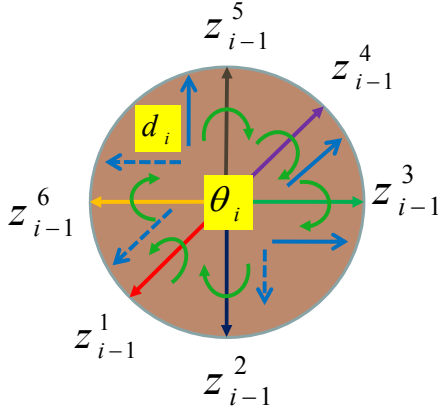
The machinery efficient workspaces of the industrial robot Fanuc LR Mate 200iC are determined by specifying the four twist angles which appear in the reconfigurable (RT)(RT)(RT)RRR kinematic model. The latter is a special case of the general 6-DOF Global Kinematic Model (GKM) (Djuric et al. 2010) in which the Denavit–Hartenberg (D-H) parameters and the reconfigurable parameters are specified. The 6-DOF GKM is first introduced in Section 4. The values of the D-H and the reconfigurable parameters in the 6-DOF GKM are specified in Section 5 to realise the reconfigurable (RT)(RT)(RT)RRR kinematic model. The machinery efficient workspaces of the industrial robot Fanuc LR Mate 200iC are then identified by specifying the twist angles. The computational details and the results are presented in Section 6. The paper concludes in Section 7.

4 Introduction to 6-DOF global kinematic model

This research focuses on the novel approach for calculating the Reconfigurable Machinery Efficient Workspace (RMEW), for a complex reconfigurable kinematic structure. This approach will capture multiple machinery efficient workspace solutions, based on different twist angles. The main focus of this study is on analysis and visualisation of multiple efficient workspaces. This calculation is based on a previously developed and validated complex reconfigurable machinery kinematic structure named n -DOF Global Kinematic Model (n -GKM) (Djuric et al., 2010).

Every joint has six vectors with different directions. These are defined with six possible joint directions (six for translation – x , y and z – positive and negative and six for rotation – around x , y and z – clockwise and counterclockwise) and are given with z_{i-1}^j in Figure 3. The number of all possible configurations in one reconfigurable joint is 48 ($C_6 = 48 * (48 - 1)^{6-1}$). The graphical representation of this joint is shown in Figure 3(Djuric et al., 2010).

Figure 3 Reconfigurable model of joint $I - 1$ (see online version for colours)



Source: Djuric et al. (2010)

The Denavit–Hartenberg (D-H) parameters for this model are shown in Table 1. In this model, each joint represents a combination of either rotational (R_i) or translational (T_i) joint types or any desired joint positive direction. The joint positive directions are determined by their twist angles (α_i), which are explained by the D-H rules (Denavit and Hartenberg, 1965). Joint variable parameters d_i (translational) and θ_i (rotational) are shown in Figure 3. Both translational and rotational joint variables are unified using two additional parameters. These parameters are d_{DHi} (link offset along previous z to the common normal – when the related joint is rotational) and θ_{DHi} (joint angle about z , from old x to new x – when the related joint is translational). Link length of the common normal is given with the parameter a_i as given in Table 1.

Table 1 D-H parameters for a 6-DOF global kinematic model

i	d_i	θ_i	a_i	α_i
1	$R_1 d_{DH1} + T_1 d_1$	$R_1 \theta_1 + T_1 \theta_{DH1}$	a_1	$0^\circ, \pm 180^\circ, \pm 90^\circ$
2	$R_2 d_{DH2} + T_2 d_2$	$R_2 \theta_2 + T_2 \theta_{DH2}$	a_2	$0^\circ, \pm 180^\circ, \pm 90^\circ$
3	$R_3 d_{DH3} + T_3 d_3$	$R_3 \theta_3 + T_3 \theta_{DH3}$	a_3	$0^\circ, \pm 180^\circ, \pm 90^\circ$
4	$R_4 d_{DH4} + T_4 d_4$	$R_4 \theta_4 + T_4 \theta_{DH4}$	a_4	$0^\circ, \pm 180^\circ, \pm 90^\circ$
5	$R_5 d_{DH5} + T_5 d_5$	$R_5 \theta_5 + T_5 \theta_{DH5}$	a_5	$0^\circ, \pm 180^\circ, \pm 90^\circ$
6	$R_6 d_{DH6} + T_6 d_6$	$R_6 \theta_6 + T_6 \theta_{DH6}$	a_6	$0^\circ, \pm 180^\circ, \pm 90^\circ$

A serial link manipulator represents a series of links, which connect the end-effector to the base, with each link connected to the next by an actuated joint. If a group of coordinate frames are attached to each link, the relationship

between two links can be described with a homogeneous transformation matrix using D-H parameters from Table 1. They are named ${}^{i-1}A_i$, where i is the number of joints ($i = 1, 2, \dots, n$). We have equation (1):

$${}^{i-1}A_i = \begin{bmatrix} \cos(R_i \theta_i + T_i \theta_{DHi}) & -K_{Ci} \sin(R_i \theta_i + T_i \theta_{DHi}) & 0 & 0 & K_{Si} \sin(R_i \theta_i + T_i \theta_{DHi}) & a_i \cos(R_i \theta_i + T_i \theta_{DHi}) \\ \sin(R_i \theta_i + T_i \theta_{DHi}) & K_{Ci} \cos(R_i \theta_i + T_i \theta_{DHi}) & 0 & 0 & -K_{Si} \cos(R_i \theta_i + T_i \theta_{DHi}) & a_i \sin(R_i \theta_i + T_i \theta_{DHi}) \\ 0 & 0 & K_{Si} & 0 & 0 & 0 \\ 0 & 0 & 0 & K_{Ci} & 0 & 0 \\ K_{Si} \sin(R_i \theta_i + T_i \theta_{DHi}) & a_i \cos(R_i \theta_i + T_i \theta_{DHi}) & 0 & 0 & R_i d_{DHi} + T_i d_i & 1 \\ -K_{Si} \cos(R_i \theta_i + T_i \theta_{DHi}) & a_i \sin(R_i \theta_i + T_i \theta_{DHi}) & 0 & 0 & 0 & 1 \end{bmatrix} \quad (1)$$

5 The machinery-efficient workspace calculation

The reconfigurable parameters in the model which determine joint type and control sine and cosine of the twist angles are given as the following:

Rotational joint values:

$$R_i = 1 \text{ and } T_i = 0 \quad (2)$$

Translational joint values:

$$R_i = 0 \text{ and } T_i = 1 \quad (3)$$

$$R_{Si} = \sin \alpha_i \quad (4)$$

$$K_{Ci} = \cos \alpha_i \quad (5)$$

The reconfigurable machinery can now be kinematically modelled by using the link transforms:

$${}^0A_n = {}^0A_1 A_2^2 A_3^3 \dots {}^{n-1}A_n \quad (6)$$

where 0A_n is the pose matrix of the end-effector relative to base; ${}^{i-1}A_{n1}$ is the link transform for the i th joint and n is the number of links. In this case of six reconfigurable joints, n is six. From the 6-GKM model, the most significant reconfigurable kinematic structure has been selected and named reconfigurable efficient workspace calculation for an (RT)(RT)(RT)RRR robot kinematic structure (see Figure 4). The related D-H parameters are given in Table 2.

This model is a subset of the full reconfigurable model presented in Table 1. These kinematic structures are related to each other and connected using the pre-determined reconfigurable parameters given in Table 3. There are two categories of reconfigurable parameters. The twist angle's sine control parameter (K_{Si}) and the twist angle's cosines control parameter (K_{Ci}) are used to control sine and cosine of the twist angles. These parameters are calculated using equations (4) and (5) and the twist angle values given in Table 2. Secondly, R_i and T_i which are used to control joints type (translational and/or rotational) are given in equations (2) and (3). The reconfigurable parameters of the reconfigurable (RT)(RT)(RT)RRR machinery kinematic structure are summarised in Table 3.

Figure 4 Reconfigurable (RT)(RT)(RT)RRR machinery kinematic structure (see online version for colours)

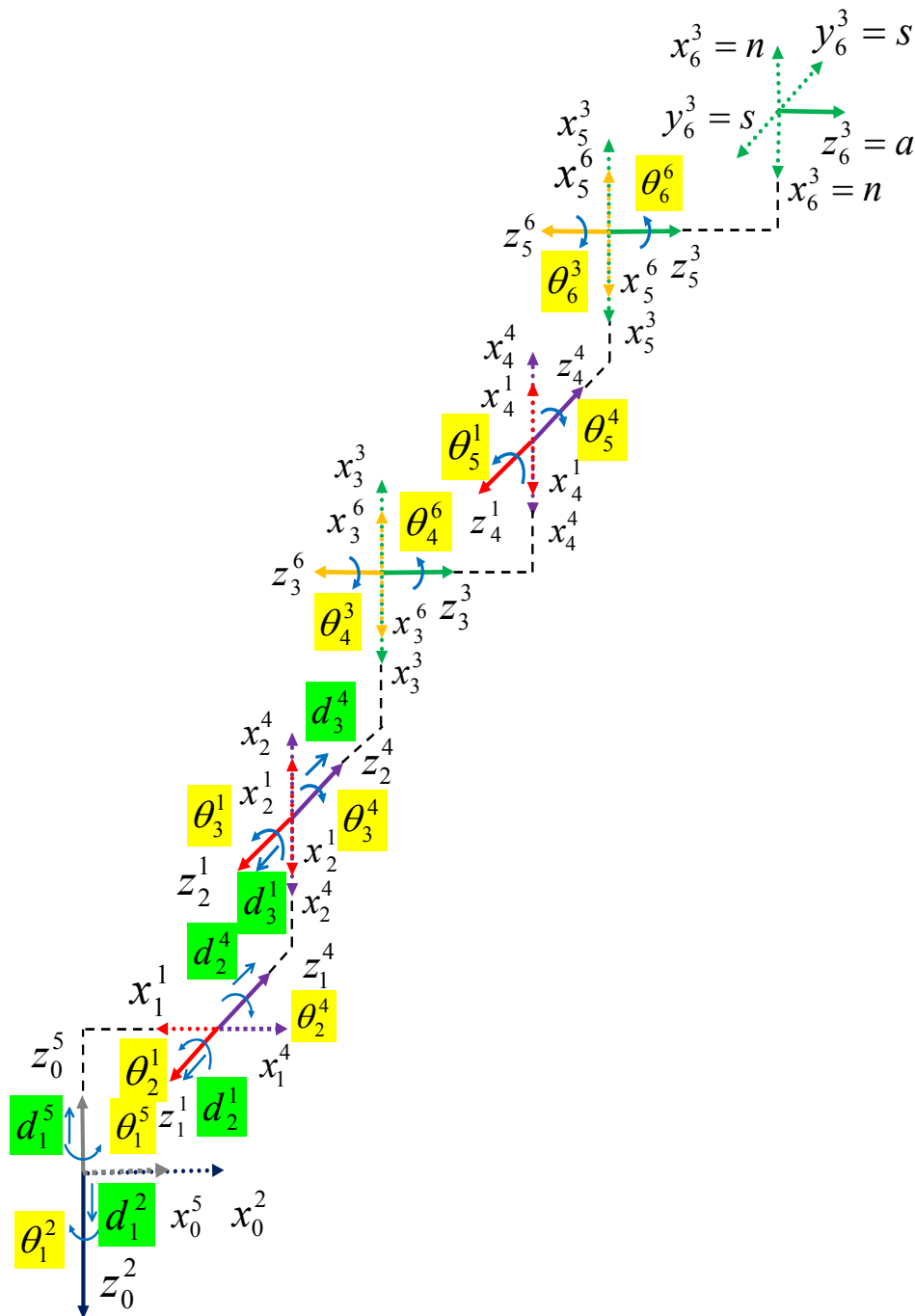


Table 2 D-H parameters for (RT)(RT)(RT)RRR model

i	d_i	θ_i	a_i	α_i
1	$R_1 d_{DH1} + T_1 d_1$	$R_1 \theta_1 + T_1 \theta_{DH1}$	a_1	$\pm 90^\circ$
2	$R_2 d_{DH2} + T_2 d_2$	$R_2 \theta_2 + T_2 \theta_{DH2}$	a_2	$0^\circ, \pm 180^\circ$
3	$R_3 d_{DH3} + T_3 d_3$	$R_3 \theta_3 + T_3 \theta_{DH3}$	a_3	$\pm 90^\circ$
4	d_{DH4}	θ_4	a_4	$\pm 90^\circ$
5	d_{DH5}	θ_5	a_5	$\pm 90^\circ$
6	d_{DH6}	θ_6	a_6	$0^\circ, \pm 180^\circ$

Table 3 Reconfigurable Parameters for (RT)(RT)(RT)RRR machinery kinematic structure

i	Sine control values	Cosine control values	R_i	T_i
1	$K_{S1} = \pm 1$	$K_{C1} = 0$	1	1
2	$K_{S2} = 0$	$K_{C2} = \pm 1$	1	1
3	$K_{S3} = \pm 1$	$K_{C3} = 0$	1	1
4	$K_{S4} = \pm 1$	$K_{C4} = 0$	1	0
5	$K_{S5} = \pm 1$	$K_{C5} = 0$	1	0
6	$K_{S6} = 0$	$K_{C6} = \pm 1$	1	0

The homogeneous transformation matrices for the (RT)(RT)(RT)RRR machinery kinematic structure are

$${}^0A_1 = \begin{bmatrix} \cos(R_1\theta_1 + T_1\theta_{DH1}) & 0 & K_{S1} \sin(R_1\theta_1 + T_1\theta_{DH1}) & a_1 \cos(R_1\theta_1 + T_1\theta_{DH1}) \\ \sin(R_1\theta_1 + T_1\theta_{DH1}) & 0 & -K_{S1} \cos(R_1\theta_1 + T_1\theta_{DH1}) & a_1 \sin(R_1\theta_1 + T_1\theta_{DH1}) \\ 0 & K_{S1} & 0 & R_1 d_{DH1} + T_1 d_1 \\ 0 & 0 & 0 & 1 \end{bmatrix} \quad (7)$$

$${}^1A_2 = \begin{bmatrix} \cos(R_2\theta_2 + T_2\theta_{DH2}) & -K_{C2} \sin(R_2\theta_2 + T_2\theta_{DH2}) & 0 & a_2 \cos(R_2\theta_2 + T_2\theta_{DH2}) \\ \sin(R_2\theta_2 + T_2\theta_{DH2}) & K_{C2} \cos(R_2\theta_2 + T_2\theta_{DH2}) & 0 & a_2 \sin(R_2\theta_2 + T_2\theta_{DH2}) \\ 0 & 0 & K_{C2} & R_2 d_{DH2} + T_2 d_2 \\ 0 & 0 & 0 & 1 \end{bmatrix} \quad (8)$$

$${}^2A_3 = \begin{bmatrix} \cos(R_3\theta_3 + T_3\theta_{DH3}) & 0 & K_{S3} \sin(R_3\theta_3 + T_3\theta_{DH3}) & a_3 \cos(R_3\theta_3 + T_3\theta_{DH3}) \\ \sin(R_3\theta_3 + T_3\theta_{DH3}) & 0 & -K_{S3} \cos(R_3\theta_3 + T_3\theta_{DH3}) & a_3 \sin(R_3\theta_3 + T_3\theta_{DH3}) \\ 0 & K_{S3} & 0 & R_3 d_{DH3} + T_3 d_3 \\ 0 & 0 & 0 & 1 \end{bmatrix} \quad (9)$$

$${}^3A_4 = \begin{bmatrix} \cos(\theta_4) & 0 & K_{S4} \sin(\theta_4) & a_4 \cos(\theta_4) \\ \sin(\theta_4) & 0 & -K_{S4} \cos(\theta_4) & a_4 \sin(\theta_4) \\ 0 & K_{S4} & 0 & d_{DH4} \\ 0 & 0 & 0 & 1 \end{bmatrix} \quad (10)$$

$${}^4A_5 = \begin{bmatrix} \cos(\theta_5) & 0 & K_{S5} \sin(\theta_5) & a_5 \cos(\theta_5) \\ \sin(\theta_5) & 0 & -K_{S5} \cos(\theta_5) & a_5 \sin(\theta_5) \\ 0 & K_{S5} & 0 & d_{DH5} \\ 0 & 0 & 0 & 1 \end{bmatrix} \quad (11)$$

$${}^5A_6 = \begin{bmatrix} \cos(\theta_6) & -K_{C6} \sin(\theta_6) & 0 & a_6 \cos(\theta_6) \\ \sin(\theta_6) & K_{C6} \cos(\theta_6) & 0 & a_6 \sin(\theta_6) \\ 0 & 0 & K_{C6} & d_{DH6} \\ 0 & 0 & 0 & 1 \end{bmatrix} \quad (12)$$

The calculation of the 2D end-effector orientation space is dependent on the three joint angles: Joint 2, Joint 3 and Joint 5. A formula for Joint 5 is generated by assigning the initial angular positions for Joint 1, Joint 4 and Joint 6 in the forward kinematic solution. Equations (8) and (9) are used to determine Joint 1 at its initial position based upon values given in Table 3:

$$K_{\cos\theta_1} = \cos\theta_1 \quad (13)$$

$$K_{\sin\theta_1} = 0 \quad (14)$$

Equation (7) is combined with equations (13) and (14) and the new homogeneous transformation matrix related to Joint 1 is calculated and presented in equation (15):

$${}^0A_1 = \begin{bmatrix} K_{\cos\theta_1} & 0 & 0 & a_1 K_{\cos\theta_1} \\ 0 & 0 & -K_{S1} K_{\cos\theta_1} & 0 \\ 0 & K_{S1} & 0 & R_1 d_{DH1} + T_1 d_1 \\ 0 & 0 & 0 & 1 \end{bmatrix} \quad (15)$$

Similarly, combining equations (10), (16) and (17), the new homogeneous transformation matrix related to Joint 4 is calculated and presented in equation (18):

$$K_{\cos\theta_4} = \cos\theta_4 \quad (16)$$

$$K_{\sin\theta_4} = 0 \quad (17)$$

$${}^3A_4 = \begin{bmatrix} K_{\cos\theta_4} & 0 & 0 & a_4 K_{\cos\theta_4} \\ 0 & 0 & -K_{S4} K_{\cos\theta_4} & 0 \\ 0 & K_{S4} & 0 & d_{DH4} \\ 0 & 0 & 0 & 1 \end{bmatrix} \quad (18)$$

Combining equations (12), (19) and (20), the new homogeneous transformation matrix related to Joint 6 is calculated and presented in equation (21):

$$K_{\cos\theta_6} = \cos\theta_6 \quad (19)$$

$$K_{\sin\theta_6} = 0 \quad (20)$$

$${}^5A_6 = \begin{bmatrix} K_{\cos\theta_6} & 0 & 0 & a_6 K_{\cos\theta_6} \\ 0 & K_{C6} K_{\cos\theta_6} & 0 & 0 \\ 0 & 0 & K_{C6} & d_{DH6} \\ 0 & 0 & 0 & 1 \end{bmatrix} \quad (21)$$

The rotational matrices for the (RT)(RT)(RT)RRR machinery kinematic structure are shown below:

$${}^0R_1 = \begin{bmatrix} K_{\cos\theta_1} & 0 & 0 \\ 0 & 0 & -K_{S1} K_{\cos\theta_1} \\ 0 & K_{S1} & 0 \end{bmatrix} \quad (22)$$

$${}^1R_2 = \begin{bmatrix} \cos(R_2\theta_2 + T_2\theta_{DH2}) - K_{C2} \sin(R_2\theta_2 + T_2\theta_{DH2}) & 0 \\ \sin(R_2\theta_2 + T_2\theta_{DH2}) & K_{C2} \cos(R_2\theta_2 + T_2\theta_{DH2}) & 0 \\ 0 & 0 & K_{C2} \end{bmatrix} \quad (23)$$

$${}^2R_3 = \begin{bmatrix} \cos(R_3\theta_3 + T_3\theta_{DH3}) & 0 & K_{S3} \sin(R_3\theta_3 + T_3\theta_{DH3}) \\ \sin(R_3\theta_3 + T_3\theta_{DH3}) & 0 & -K_{S3} \cos(R_3\theta_3 + T_3\theta_{DH3}) \\ 0 & K_{S3} & 0 \end{bmatrix} \quad (24)$$

$${}^3R_4 = \begin{bmatrix} K_{\cos\theta_4} & 0 & 0 \\ 0 & 0 & -K_{S4}K_{\cos\theta_4} \\ 0 & K_{S4} & 0 \end{bmatrix} \quad (25)$$

$${}^4R_5 = \begin{bmatrix} \cos(\theta_5) & 0 & K_{S5} \sin(\theta_5) \\ \sin(\theta_5) & 0 & -K_{S5} \cos(\theta_5) \\ 0 & K_{S5} & 0 \end{bmatrix} \quad (26)$$

$${}^5R_6 = \begin{bmatrix} K_{\cos\theta_6} & 0 & 0 \\ 0 & K_{C6}K_{\cos\theta_6} & 0 \\ 0 & 0 & K_{C6} \end{bmatrix} \quad (27)$$

By observing the homogeneous matrices, it is clear that the majority of the complexity of the model is involved in Joint 2 and Joint 3 (see equations 22–27). The relation between Joint 2 and Joint 3 is expressed and simplified using the following two equations:

$$\begin{aligned} & \sin(R_i\theta_i + T_i\theta_{DH_i}) \cos(R_{(i+1)}\theta_{(i+1)} + T_{(i+1)}\theta_{DH(i+1)}) \\ & + K_{C_i} \cos(R_i\theta_i + T_i\theta_{DH_i}) \sin(R_{(i+1)}\theta_{(i+1)} + T_{(i+1)}\theta_{DH(i+1)}) \\ & + \sin(R_i\theta_i + T_i\theta_{DH_i} + K_{C_i}(R_{(i+1)}\theta_{(i+1)} + T_{(i+1)}\theta_{DH(i+1)})) \end{aligned} \quad (28)$$

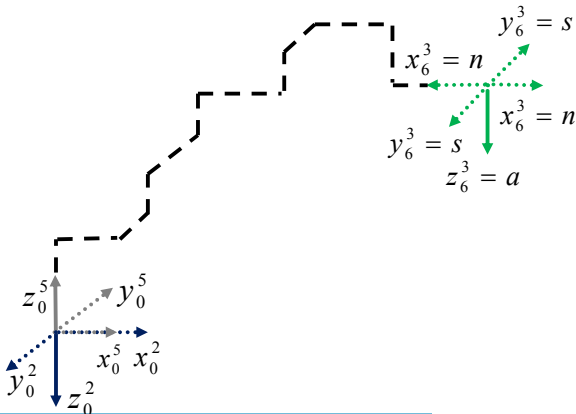
$i = 1, 2, \dots, 6$

$$\begin{aligned} & \cos(R_i\theta_i + T_i\theta_{DH_i}) \cos(R_{(i+1)}\theta_{(i+1)} + T_{(i+1)}\theta_{DH(i+1)}) \\ & - K_{C_i} \sin(R_i\theta_i + T_i\theta_{DH_i}) \sin(R_{(i+1)}\theta_{(i+1)} + T_{(i+1)}\theta_{DH(i+1)}) \\ & = \cos(R_i\theta_i + T_i\theta_{DH_i} + K_{C_i}(R_{(i+1)}\theta_{(i+1)} + T_{(i+1)}\theta_{DH(i+1)})) \end{aligned} \quad (29)$$

$i = 1, 2, \dots, 6$

The tool perpendicularity condition is shown in Figure 5. The reason that this condition was selected is that it is of prime importance in many manufacturing operations such as: painting, water jet cutting, material deposition, etc.

Figure 5 Reconfigurable (RT)(RT)(RT)RRR machinery perpendicularity condition (see online version for colours)



The tool frame vectors n , s and a (normal, sliding and approach) will always be perpendicular to the floor, with the approach vector pointing down if equation (30) is satisfied:

$${}^0R_6 = \begin{bmatrix} r_{11} & 0 & 0 \\ 0 & r_{22} & 0 \\ 0 & 0 & r_{33} \end{bmatrix} = \begin{bmatrix} n_x & s_x & a_x \\ n_y & s_y & a_y \\ n_z & s_z & a_z \end{bmatrix} \quad (30)$$

The three matrix elements r_{11} , r_{22} and r_{33} are determined in equation (31). Equation (31) satisfies the perpendicularity condition presented in Figure 5 and can be visually validated:

$${}^0R_6 = \begin{bmatrix} \pm 1 & 0 & 0 \\ 0 & \pm 1 & 0 \\ 0 & 0 & \mp 1 \end{bmatrix} \quad (31)$$

To force the tool frame to be perpendicular to the floor all the time, the reconfigurable rotational matrix has been calculated first in equation (32):

$${}^0R_6 = {}^0R_1 {}^1R_2 {}^2R_3 {}^3R_4 {}^4R_5 {}^5R_6 \quad (32)$$

Joint angles 2 and 3 will vary between their limits, while Joint 5 is calculated by forcing rotational matrix 0R_6 to satisfy the orientation condition given in equation (30). Joint 5 is expressed in a reconfigurable manner and can be used for the efficient workspace analysis based on the twist angle's alpha (see equation 33):

$$\theta_5 = a \tan 2 \frac{-r_{33}K_{s1}K_{4\cos} \sin(R_2\theta_2 + T_2\theta_{DH2}) + K_{c2}(R_3\theta_3 + T_3\theta_{DH3})}{r_{33}K_{s1}K_{c2}K_{s3}K_{s4}K_{6\cos} \cos(R_2\theta_2 + T_2\theta_{DH2} + K_{c2}(R_3\theta_3 + T_3\theta_{DH3}))} \quad (33)$$

6 Analysis of the machinery efficient workspace based on the twist angles for the Fanuc LR Mate 200iC robot

The calculated Joint 5 in equation (33) depends only on some of the twist angle control parameters, K_{S1} , K_{S3} , K_{S4} and K_{C2} , and joint angle control parameters $K_{4\cos}$ and $K_{6\cos}$. The application of the 6-DOF GKM for machinery efficient workspace, presented in this paper, is applied on a Fanuc LR Mate 200iC kinematic structure as a reference model, as shown in Figure 6 and Table 4. All joints in this robot are rotational. Hence, all values of rotational parameters (R_i) have a value of 1 and all translational parameters (T_i) have a value of 0.

If a coordinate frame is attached to each link, the relationship between two links can be described using the Denavit and Hartenberg rules (12) and the four related parameters presented in Table 5. Dimensions are in millimetres (Fanuc, 2009).

For the fixed three joints, $\theta_{DH1} = 0^\circ$ or 180° , $\theta_{DH4} = 0^\circ$ or 180° , $\theta_{DH6} = 0^\circ$ or 180° , and the tool perpendicularity

condition, using the formula for Joint 5 in equation (33), a 2D Fanuc LR Mate 200iC robot efficient workspace is calculated and presented together with the related workspace in Figure 7. This explains the difference between robot workspace and its efficient workspace related to desired applications. The workspace represents complete robot reachable space calculated without considering the end-effector orientation. The robot workspace will change when the end-effector orientation is included in calculation and limited by the selected application. Such a new space is called efficient workspace and it has a different shape. It is always smaller than the complete workspace. The presented efficient workspace is static, which means that the desired tool orientation is always fixed, perpendicular to the robot's base. The future research direction is to calculate the dynamic efficient workspace which would allow the change of the tool orientation.

Figure 6 Fanuc LR Mate 200iC robot kinematic structure (see online version for colours)

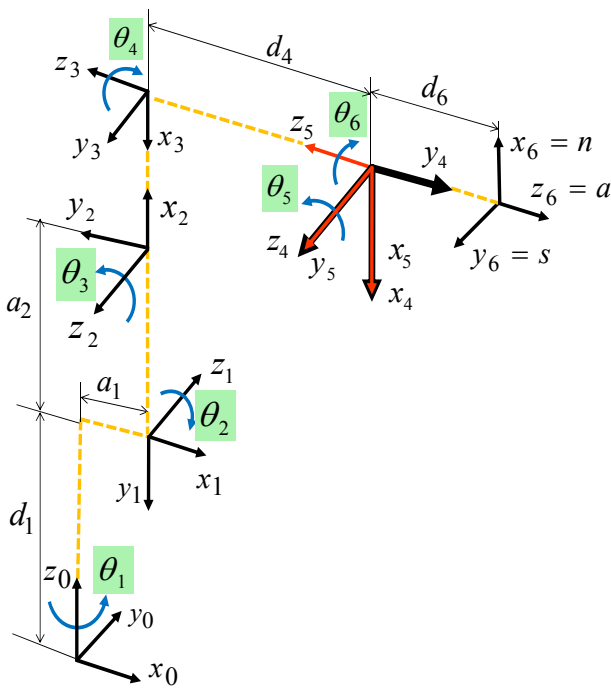


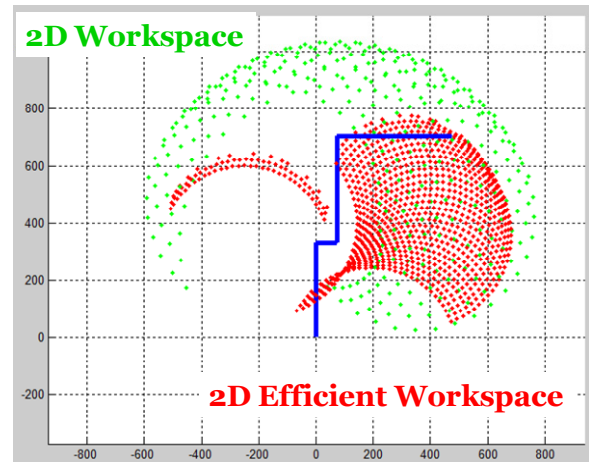
Table 4 Reconfigurable parameters for the Fanuc LR Mate 200iC kinematic structure

i	Sine control values	Cosine control values	R_i	T_i
1	$K_{S1} = -1$	$K_{C1} = 0$	1	0
2	$K_{S2} = 0$	$K_{C2} = -1$	1	0
3	$K_{S3} = 1$	$K_{C3} = 0$	1	0
4	$K_{S4} = -1$	$K_{C4} = 0$	1	0
5	$K_{S5} = 1$	$K_{C5} = 0$	1	0
6	$K_{S6} = 0$	$K_{C6} = 1$	1	0

Table 5 D-H parameters for Fanuc LR Mate 200iC

i	Sine control values	Cosine control values	R_i	T_i
1	$K_{S1} = -1$	$K_{C1} = 0$	1	0
2	$K_{S2} = 0$	$K_{C2} = -1$	1	0
3	$K_{S3} = 1$	$K_{C3} = 0$	1	0
4	$K_{S4} = -1$	$K_{C4} = 0$	1	0
5	$K_{S5} = 1$	$K_{C5} = 0$	1	0
6	$K_{S6} = 0$	$K_{C6} = 1$	1	0

Figure 7 Fanuc LR Mate 200iC robot workspace and efficient workspace (see online version for colours)



Both spaces are calculated for the linked Joint 2 and Joint 3, in equation (34):

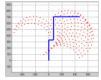
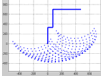
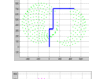
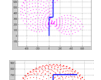
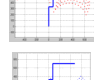
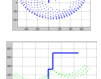
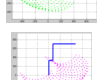
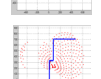

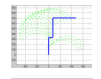
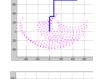
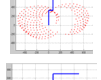
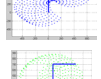
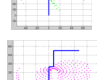
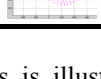
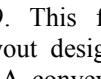
$$\text{Joint}_{23\text{Limit_min}} \leq (\theta_2 + \theta_3) \leq \text{Joint}_{23\text{Limit_max}} \tag{34}$$

The Fanuc LR Mate 200iC efficient workspace depends on four reconfigurable parameters K_{S1} , K_{C2} , K_{S3} and K_{S4} .

To show the significance of the reconfigurable modelling method and its applications, all possible values of the four reconfigurable parameters are used for generating different efficient workspaces. The twist angle's possible values are 0° , $\pm 180^\circ$, $\pm 90^\circ$. The related reconfigurable parameter values are +1 or -1. There are 16 different combinations presented in Table 6.

The graphical representations of all 16 different efficient workspaces are shown via MATLAB tools in Table 6. The analysis is made for the fixed link lengths and link offsets used from the Fanuc LR Mate 200iC robot. By observing Table 6, it is clear that for $\alpha_1 = -90^\circ$ the efficient workspace is in the upper area. See cases 1, 3, 4, 5, 9, 10, 11 and 15. For $\alpha_1 = 90^\circ$, the efficient workspace is in the lower area. See cases 2, 6, 7, 8, 12, 13, 14 and 16. The presented calculation and visualisation of the efficient workspace show that its shape and position can be controlled by the twist angles.

Table 6 Efficient workspace analysis with respect to the twist angles α_i (see online version for colours)

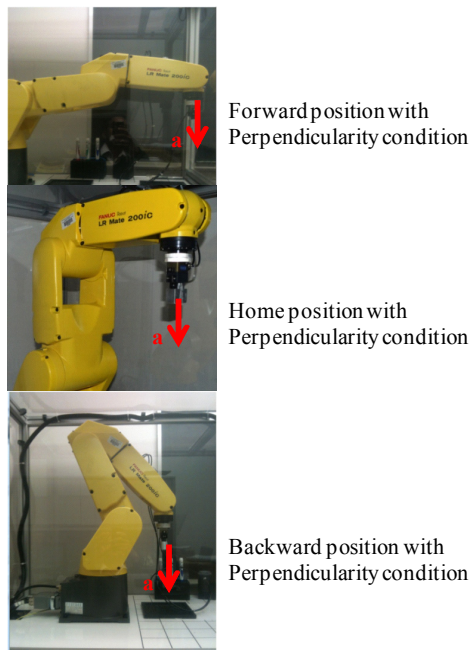
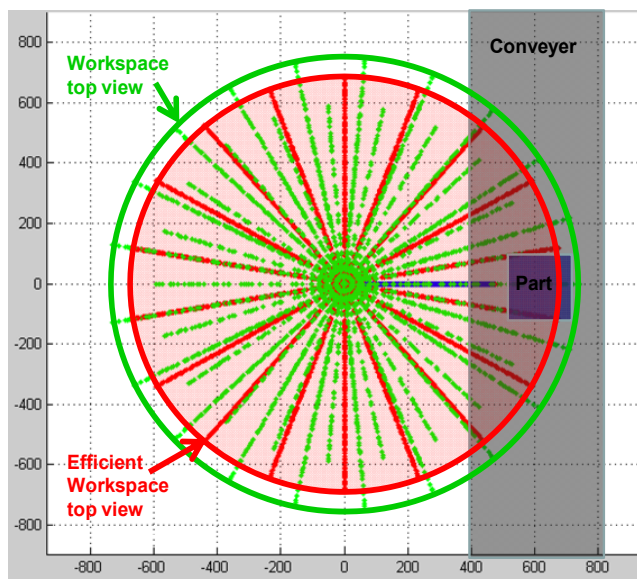
	α_1	α_2	α_3	α_4	K_{S1}	K_{C2}	K_{S3}	K_{S4}	Work window
1	-90°	180°	90°	-90°	-1	-1	1	-1	
2	-90°	180°	90°	-90°	1	-1	1	-1	
3	-90°	0°	90°	-90°	-1	1	1	-1	
4	-90°	180°	-90°	-90°	-1	-1	-1	-1	
5	-90°	180°	90°	90°	-1	-1	1	1	
6	90°	0°	90°	-90°	1	1	1	-1	
7	90°	180°	-90°	-90°	1	-1	-1	-1	
8	90°	180°	90°	90°	1	-1	1	1	
9	-90°	0°	-90°	-90°	-1	1	-1	-1	
10	-90°	0°	90°	90°	-1	1	1	1	
11	-90°	180°	-90°	90°	-1	-1	-1	1	
12	90°	0°	-90°	-90°	1	1	-1	-1	
13	90°	0°	90°	90°	1	1	1	1	
14	90°	180°	-90°	90°	1	-1	-1	1	
15	-90°	0°	-90°	90°	-1	1	-1	1	
16	90°	0°	-90°	90°	1	1	-1	1	

The presented methodology is applicable for calculation of the efficient workspaces of any reconfigurable kinematic model. It can be used for the design of a new kinematic structure related to the desired application(s). A quick comparison between existing kinematic structures can be done through the unified reconfigurable model and selection can be based on the shape and position of the efficient workspace.

Several positions of the Fanuc robot with the approach vector pointing down have been created and used for model validation, as shown in Figure 8.

The layout design using efficient workspace Fanuc LR Mate 200iC robot is shown in Figure 9.

The application of the research findings is illustrated through the example shown in Figure 9. This figure represents a segment of the production layout design. A robot is placed in the centre of the circle. A conveyor is placed on its right-hand side. The main assumption is that the robot needs to operate within the part which is moving on the conveyor, as shown in Figure 9. The part is within the robot's workspace, but it is outside the robot's efficient workspace. This example provides a visualisation of the efficient workspace and shows that the robot can reach a part but is not able to operate for the desired application. Hence, visualisation of the robot's efficient workspace/s will serve as a design tool in production line planning for one or multiple industrial robots.

Figure 8 Fanuc LR Mate 200iC robot approach vector pointing down**Figure 9** Layout design using efficient workspace Fanuc LR Mate 200iC (see online version for colours)

7 Conclusion

A novel methodology for calculation, visualisation and analysis of the RMEW based on the twist angles has been presented and demonstrated through an example of the Fanuc LR Mate 200iC robot.

The (RT)(RT)(RT)RRR reconfigurable machinery kinematic structure is selected from the n -GKM model and applied to the Fanuc LR Mate 200iC robot. The reconfigurable parameters are picked such as that the model unifies different twist angles (joint positive direction) and

different joint types (rotational and/or translational). Using the forward kinematic solution where Joints 1, 4 and 6 are fixed, a 2D reconfigurable efficient workspace is calculated. This space is described such that Joints 2 and 3 vary between their limits, while Joint 5 is calculated to follow the perpendicularity condition. The calculations show that Joint 5's angular position depends on only four reconfigurable parameters: K_{S1} , K_{C2} , K_{S3} and K_{S4} . These parameters control the sine and cosine of the first four joints.

All 16 possible combinations for four reconfigurable parameters (K_{S1} , K_{C2} , K_{S3} and K_{S4}) are used for the efficient workspace generation of the Fanuc LR Mate 200iC robot example. The visual outcomes of different efficient workspace shapes show that tool orientation significantly depends on the machinery joints' positive directions (twist angles).

This RMEW can be used as a design tool for new machinery kinematic structure. Because of its reconfigurable nature, it can be used as an efficient tool for selection of the optimal machine configurations for the desired tool orientation. This is an efficient tool for quick and accurate layout design, product design and production planning. The efficient workspace can help quickly and accurately locate the devices in the work cell. The example of placing the conveyer and parts to be reachable by the robot with a perpendicular tool is shown in Figure 9. The part is inside the robot workspace, but it is still not reachable because of the tool's orientation. This efficient workspace tool helps to solve similar problems.

References

- Brogårdh, T. (2007) 'Present and future robot control development: an industrial perspective', *Annual Reviews in Control*, Vol. 31, No. 1, pp.69–79.
- Castelli, G., Ottaviano, E. and Ceccarelli, M. (2008) 'A fairly general algorithm to evaluate workspace characteristics of serial and parallel manipulators #', *Mechanics Based Design of Structures and Machines*, Vol. 36, No. 1, pp.14–33.
- Cebula, A.J. and Zsombor-Murray, P.J. (2006) 'Formulation of the workspace equation for wrist-partitioned spatial manipulators', *Mechanisms and Machine Theory*, Vol. 41, pp.778–789.
- Ceccarelli, M. and Lanni, C. (2003) 'A multi-objective optimum design of general 3R manipulators for prescribed workspace limits', *Mechanisms and Machine Theory*, Vol. 39, pp.119–132.
- Curkovic, P., Jerbic, B. and Stipanovic, T. (2013) 'Coordination of robots with overlapping workspaces based on motion co-evolution', *International Journal of Simulation Modelling*, Vol. 12, No. 1, pp.27–38.
- Denavit, J. and Hartenberg, R.S. (1965) 'A kinematic notation for lower-pair mechanisms based on matrices', *ASME Journal of Applied Mechanics*, Vol. 22, No. 2, pp.215–221.
- Djuric, A.M. and ElMaraghy, W.H. (2008) 'Filtering boundary points of the robot workspace', *Conference Proceedings of the 5th International Conference on Digital Enterprise Technology*, 22–24 October, Nantes, France, pp.597–608.

- Djuric, A.M. and Urbanic, R.J. (2009) 'A methodology for defining the efficient space (work window) for a machine configuration', *Proceedings of the 3rd International Conference on Changeable, Agile, Reconfigurable and Virtual Production*, 5–7 October, Munich, Germany.
- Djuric, A.M., Al Saida, R. and ElMaraghy, W. (2010) 'Global kinematic model generation for n -DOF reconfigurable machinery structure', *Proceedings of the IEEE Conference on Automation Science and Engineering*, 21–24 August, Toronto, ON, pp.804–809.
- Djuric, A.M., Filipovic, M., and Chen, W. (2013a), 'Visualization of the three critical spaces related to the 6-DOF machinery', *Proceedings of the 4th International Congress of Serbian Society of Mechanics*, 3–7 June, Vrnjacka Banja, Serbia.
- Djuric, A.M., Filipovic, M. and Kevac, L. (2013b) 'Graphical representation of the significant 6R KUKA robots space', *Proceedings of the 11th Symposium on Intelligent Systems and Informatics*, 26–28 September, Subotica, Serbia, pp.221–226.
- Djuric, A.M., Urbanic, R.J., Filipovic, M. and Kevac, L. (2013c) 'Effective work region visualization for serial 6 DOF robots', *Proceedings of the 5th International Conference on Changeable, Agile, Reconfigurable and Virtual Production*, 6–9 October, Munich, Germany, pp.207–212.
- Fanuc, I. (2009) *LR Mate[®] 2000iC Series & R-30iATM Mate Controller*. Available online at: https://moodle.polymtl.ca/pluginfile.php/101696/mod_resource/content/0/LR-Mate-200iC-Series_-R-30iA-Mate-Controller.pdf.
- Foitzik, B. (2014) *Mensch-Roboter-Kooperation: Mit Kollege Roboter' im Fusionsreaktor [Human-robot cooperation: with, friendly robot 'in a fusion reactor']*. Available online at: <http://www.produktion.de/automatisierung/mensch-roboter-kooperation-mit-kollege-roboter-im-fusionsreaktor/> (accessed on 21 April 2014) (in German).
- Guerra-Zubiaga, D.A., Rios, E., Parkin, R., Jackson, M., Tomovic, M.M., Ramirez-Mendoza, R. (2010) 'Mechatronics design methodology applied at manufacturing companies', *International Journal of Manufacturing Technology and Management*, Vol. 19, No. 3, pp.191–210.
- Haque, B. (2012) 'Overcoming the challenges of automating and integrating virtual product development processes', *International Journal of Computer Applications in Technology*, Vol. 44, No. 1, pp.1–11.
- Koren, Y. and Shpitalni, M. (2010) 'Design of reconfigurable manufacturing systems', *Journal of Manufacturing Systems*, Vol. 29, No. 4, pp.130–141.
- van Amerongen, J. and Breedveld, P. (2003) 'Modelling of physical systems for the design and control of mechatronic systems', *Annual Reviews in Control*, Vol. 27, No. 1, pp.87–117.
- Yan, F., Zhuang, Y. and Wang, W. (2012) 'Mobile robot 3D map building and path planning based on multi-sensor data fusion', *International Journal of Computer Applications in Technology*, Vol. 44, No. 4, pp.276–283.
- Yang, J., Yu, W., Kim, J. and Abdel-Malek, K. (2009) 'On the placement of open-loop robotic manipulators for reachability', *Mechanism and Machine Theory*, Vol. 44, pp.671–684.

Nomenclature

RMEW	Reconfigurable machinery efficient workspace
n -GKM	n -DOF global kinematic model
${}^{i-1}R_i$	Rotational matrices
d_i	Link offset along previous z to the common normal
d_{DH_i}	Link offset along previous z to the common normal (when the related joint is rotational)
θ_i	Joint angle about z , from old x to new x
θ_{DH_i}	Joint angle about z , from old x to new x (when the related joint is translation)
a_i	Link length of the common normal
α_i	Twist angle about common normal
R_i	Joints type control parameters (rotational)
T_i	Joints type control parameters (translational)
K_{Si}	Twist angle sine control parameter
K_{Ci}	Twist angle cosines control parameter
$K_{\sin\theta_i}$	Joint angle sine control parameter
$K_{\cos\theta_i}$	Joint angle cosines control parameter
n	Normal vector
s	Sliding vector
a	Approach vector
z_{i-1}^j	Axis of joint rotation/translation